Journal of Materials Chemistry B

PAPER

View Article Online
View Journal

Cite this: DOI: 10.1039/c7tb03089d

A reversible frequency upconversion probe for real-time intracellular lysosome-pH detection and subcellular imaging†

Zhe Dong, Qingxin Han, Zuolin Mou, Ge Li and Weisheng Liu *

Received 28th November 2017,
Accepted 26th January 2018

DOI: 10.1039/c7tb03089d

rsc.li/materials-b

Lysosomal pH is known to be acidic, which plays a vital role in various processes in living organisms. Frequency upconversion luminescence exhibits the unique ability to convert low energy photons into high energy photons, which can be used in live samples due to its deep penetration, low tissue damage, *etc.* The development of sensitive frequency upconversion probes with a low pK_a, high sensitivity, and specific selectivity for lysosomal pH detection is of great importance. Herein, we report a novel frequency upconversion luminescence probe, **NRH-Lyso**, by conjugating the rhodamine derivative **NRH** and the lysosome targeting functional group 4-(2-aminoethyl)morpholine. **NRH-Lyso** shows a sensitive response to acidic pH and excellent selectivity in the presence of metal ions, anions, and small molecules. Due to the structural transformation of lactam ring opening and closing of **NRH-Lyso**, the probe shows an almost 80-fold enhancement in emission intensity when the pH changes from 7.0 to 4.0 under 808 nm laser excitation. The living cell imaging data reveals that **NRH-Lyso** can selectively detect lysosomal pH changes with excellent photostability and low cytotoxicity. All these features make **NRH-Lyso** a good candidate to investigate the lysosomal pH-associated physiological and pathological processes.

Introduction

Intracellular acidic pH plays various pivotal roles in various biological processes[1] such as cell growth,[2] apoptosis,[3,4] endocytosis,[5] autophagy,[6] and receptor-mediated signal transduction[7] in eukaryotic cells. Due to their ability to adjust the pH of the inner environment in cells to acidic, lysosomes are considered as one of the most important organelles. Lysosomes contain various hydrolytic enzymes, which play key roles in immunologic defense,[8] intracellular digestion,[9] and ion metabolism.[10] Furthermore, aberrant variation in the lysosomal pH can induce dysfunction in enzymes and proteins inside the lysosomes that can only exhibit activity and functions in an acidic pH environment (4.5–5.5).[11,12] According to previous studies, an abnormal change in lysosome pH can lead to several diseases such as cancer,[13] Alzheimer's disease,[14] shock,[15] and lysosome storage diseases.[15,16] Therefore, the development of an efficient way to real time monitor the lysosome pH in living cells is of importance to investigate the physiological and pathological processes.

In the past few decades, fluorescence spectrometry has attracted significant attention than other methods for pH detection due to its simple operation, high sensitivity, high selectivity, high spatial and temporal observation, fast response, and non-invasiveness in living cells or tissues.[17–28] Although numerous attempts have been made to develop intracellular pH probes,[29–43] their applications in pH detection are still limited due to the extremely limited penetration depth and strong auto-fluorescence of these methods in the ultraviolet and visible range. It has been reported that long-wavelength emissive probes can reduce the abovementioned shortcomings.[44–47] However, there still are several limitations that impede their applications in living samples including low fluorescence quantum yield, inappropriate pK_a range, and high background fluorescence.

Nowadays anti-Stokes luminescent materials, including lanthanide-doped upconversion nanoparticles and triple–triple annihilation-based materials, are good candidates for subcellular pH detection in living tissues due to their unique ability to convert longer wavelength excitation to shorter wavelength emission.[33,48–54] However, controlling the size of these materials, which will make it easy for them to pass through the cell membrane into the inner tissues while maintaining their original optical properties, is still a major challenge in biological applications.[55,56] Two-photon absorption (TPA) is another well-used anti-Stokes luminescence process in bio-detection and other bio-applications. However, the realization of TPA needs extremely

Key Laboratory of Nonferrous Metals Chemistry and Resources Utilization of Gansu Province and State Key Laboratory of Applied Organic Chemistry, College of Chemistry and Chemical Engineering, Lanzhou University, Lanzhou 730000, P. R. China. E-mail: liuws@lzu.edu.cn; Fax: +86 931 8912582; Tel: +86 931 8915151

† Electronic supplementary information (ESI) available. See DOI: 10.1039/c7tb03089d

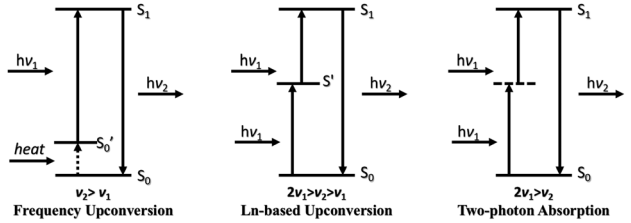

Scheme 1 Different luminescence mechanisms of FUCL (left), lanthanide upconversion (middle), and two-photon absorption (right).

high excitation energy, which limits easy and convenient applications (Scheme 1).[57,58]

Frequency upconversion luminescence (FUCL) is another attractive choice for generating anti-Stokes emission. It is characterized by continuous optical pumping from the vibrational–rotational energy sublevels of the ground states of FUCL molecules followed by the emission of radiation with a shorter wavelength.[59–62] Different from lanthanide upconversion luminescence and TPA, which occur between the zero level of the ground state (S_0) and the first excited state (S_1), FUCL starts from the thermally vibrational–rotational energy sublevels of the ground state (S_0') with the continuous absorption of pump photons accompanying the luminescence to the lowest levels of the ground state (S_0).[59,61,63–65] Notably, FUCL is a typical one photon process, and the additional energy is provided by the heat originating from the original Boltzmann distribution of dye molecules. Compared to UCNPs, the luminescent unit of FUCL is a single organic dye molecule, which is much smaller than nanoparticles and exhibits relatively higher absorptivity and tunable excitation and emission wavelengths. To date, limited examples of FUCL organic dyes have been reported,[55,66,67] and none have been applied for real-time intracellular detection of lysosomal pH and subcellular imaging.

In this study, we designed a novel FUCL lysosome pH probe, **NRH-Lyso**, *via* the chemical conjunction of the rhodamine derivative **NRH** with the lysosomal targeting group 4-(2-aminoethyl) morpholine. Li's group used **NRH** as the main skeleton of their copper probe, and it showed excellent FUCL abilities and low biotoxicity.[66,67] **NRH-Lyso** shows frequency luminescence (λ_{ex} = 808 nm) and NIR fluorescence (λ_{ex} = 685 nm) by responding to acidic pH. Detailed pH titration, reversibility, and selectivity of the probe under two excitations were systemically investigated. Furthermore, the potential applications of **NRH-Lyso** in living samples were further evaluated *via* fluorescence imaging techniques.

Experimental

Materials and methods

All chemicals were purchased from commercial suppliers and used without further purification. All solvents were of reagent grade and used without further purification unless especially noted. All reactions were monitored through thin-layer chromatography (TLC) using UV light. Benzotriazol-1-yl-oxytripyrrolidinophosphonium hexafluorophosphate (PyBOP) was purchased from Adamas Reagent Co., Ltd. Lysosome tracker Green DND-26 (LTG) was purchased from Shanghai Yeasen Biotechnology Co., Ltd. Britton–Robinson (BR) buffers were prepared by mixing 40 mM acetic acid, boric acid, and phosphoric acid. The pH of the BR buffers was adjusted by adding different amounts of diluted NaOH solution and measured by a pH-10C digital pH meter. ^{1}H NMR (400 MHz) and ^{13}C NMR (101 MHz) spectra were obtained using a Bruker AVANCE III HD 400 MHz digital NMR spectrometer with tetramethylsilane as the internal standard. Mass spectra (ESI) were obtained using an LQC system (Finngan MAT, USA) and a Bruker Daltonics Esquire 6000 mass spectrometer. All UV-vis spectra and fluorescence spectra were obtained using a Shimadzu UV-2700 spectrophotometer and a Hitachi F-7000 fluorescence spectrophotometer at room temperature, respectively. The 808 nm laser was purchased from Changchun Lslaser Co., Ltd. The DHJF-8002 low-temperature stirring reaction bath was purchased from Zhengzhou Great Wall Scientific Industrial and Trade Co., Ltd.

Synthesis and characterization of NRH

The synthetic route for **NHR** is shown in Scheme 3. Compounds **1** and **2** were obtained *via* the reported procedures.[55,66,67] Compound **1** (6-(*N*,*N*-diethylamino)-9-(2-carboxyphenyl)-1,2,3,4-tetrahydroxanthylium perchlorate, 3 mmol), compound **2** (2-(2-anilinovinyl)-1-ethyl-3,3-dimethyl-3*H*-indolium iodide, 3 mmol), and KOAc were added to a flask and dissolved in 15 mL acetic anhydride and then stirred under an argon atmosphere at 50 °C for 0.5 h. This reaction was quenched by pouring 100 mL water in the flask, and then, filtration was employed to obtain the crude product. Subsequently, the product was purified *via* silica chromatography using dichloromethane/methanol (V : V = 100 : 1 to 10 : 1) as the eluent to obtain **NRH** as a green solid. ^{1}H NMR (400 MHz, $CDCl_3$) δ (ppm): 8.14 (d, J = 8 Hz,1H), 8.04 (d, J = 12 Hz, 1H), 7.47 (m, 2H), 7.02 (t, J = 8 Hz, 2H), 6.87 (d, J = 8 Hz, 1H), 6.81 (d, J = 8 Hz, 1H), 6.55 (d, J = 8 Hz, 1H), 6.44 (s, 1H), 5.66 (d, J = 12 Hz, 1H), 3.44 (m, 6H), 2.55 (m, 6H), 1.70 (s, 6H), 1.22 (t, J = 8 Hz, 6H), 1.08 (t, J = 8 Hz, 3H). ESI-MS m/z [M^+]: 573.3.

Synthesis and characterization of NRH-Lyso

PyBOP (benzotriazol-1-yl-oxytripyrrolidinophosphonium hexafluorophosphate 0.5 mmol) was added to a solution of **NRH** (0.5 mmol) in anhydrous dichloromethane. This mixture was stirred under an argon atmosphere at 0 °C for 0.5 h. Then, 4-(2-aminoethyl) morpholine (1.0 mmol) was added dropwise to the mixture solution. The reaction mixture was left stirring at room temperature overnight. The solvent was evaporated under reduced pressure to obtain the crude product. The residue was purified through a silica gel column using petroleum/ethyl acetate (V : V = 10 : 1) to obtain **NRH-Lyso** as a yellow powder. ^{1}H NMR (400 MHz, CD_3OD) δ (ppm): 7.83 (d, J = 8 Hz, 1H), 7.58 (t, J = 8 Hz, 1H), 7.53 (d, J = 8 Hz, 2H), 7.29 (t, J = 8 Hz, 1H), 7.20 (t, J = 8 Hz, 1H), 7.14 (t, J = 8 Hz, 1H), 6.81 (d, J = 8 Hz, 1H), 6.68 (d, J = 8 Hz, 1H), 6.38 (s, 1H; d, J = 12 Hz, 1H), 6.25 (d, J = 8 Hz, 1H), 5.50 (d, 12H), 3.72 (q, J = 8 Hz, 2H), 3.58 (t, J = 8 Hz, 4H), 3.40 (q, J = 8 Hz, 6H), 2.32–2.65 (m, 8H), 1.68 (m, 6H), 1.34

(m, 4H), 1.21 (t, J = 8 Hz, 3H), 1.17 (t, J = 8 Hz, 6H). ^{13}C NMR (101 MHz, DMSO-d_6): 168.76, 156.39, 152.89, 148.85, 148.49, 144.22, 138.61, 132.52, 131.54, 128.39, 128.28, 127.55, 123.72, 123.40, 122.23, 121.32, 119.76, 119.25, 118.93, 108.45, 105.60, 104.56, 102.31, 97.14, 91.33, 67.38, 66.21, 56.02, 53.25, 5.28, 44.05, 36.42, 36.18, 27.52, 27.44, 26.61, 24.87, 22.81, 22.08, 11.58, 9.96. ESI-MS m/z [$(M + H)^+$]: 686.0.

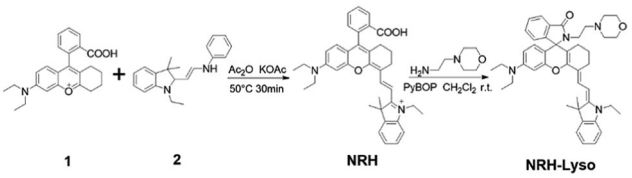

Scheme 3 Synthetic route of the lysosomal pH probe **NRH-Lyso**.

Results and discussion

Synthesis of NRH-Lyso

The lysosome pH targeting probe **NRH-Lyso** was easily synthesized in two steps, as illustrated in Scheme 2. Compounds **1** and **2** were synthesized using previously reported methods, dissolved in acetic anhydride, and heated to produce **NRH**. **NRH-Lyso** was obtained from **NRH** *via* a typical reaction with 4-(2-aminoethyl) morpholine in anhydrous CH_2Cl_2 with PyBOP as the catalyst. The final structure of **NRH-Lyso** was characterized *via* ^{1}H NMR, ^{13}C NMR, and ESI-MS.

Spectroscopic properties of NRH-Lyso to pH

The spectroscopic properties of **NRH-Lyso** were measured in Britton–Robinson (BR) buffers (40 mM) containing 1% DMSO at various pH values, and the corresponding spectra are shown in Fig. 1. The fluorescence spectra were measured under two different excitations: 685 nm and 808 nm.

The UV-vis spectra of **NRH-Lyso** at different pH values are displayed in Fig. 1a. As shown, the solution of **NRH-Lyso** was turquoise, but it changed to colorless when the pH of the BR buffer was higher than 6.0 due to the stable non-fluorescent spirolactam form of **NRH-Lyso** in an alkaline environment.

When the pH increased from 3.5 to 8.0, the broad absorption peak at 710 nm showed an intense decrease along with a weak increase in the absorption band at 390 nm. Moreover, as shown in Fig. 1b, the fluorescence spectra show a significantly enhanced NIR luminescence signal of **NRH-Lyso** at 740 nm corresponding to the H^+-induced ring opening of **NRH-Lyso**, which shows more than an 80-fold increase under 808 nm excitation; this demonstrates that **NRH-Lyso** is a highly sensitive probe under acidic conditions.

As shown in Fig. 1c, the changes in the highest fluorescence intensity (at 740 nm) of the pH titration curve could be set as a function signal of pH, which yielded a pK_a of 4.51, thus demonstrating that **NRH-Lyso** could detect lysosomal pH changes in living cells. **NRH-Lyso** also displayed excellent linearity

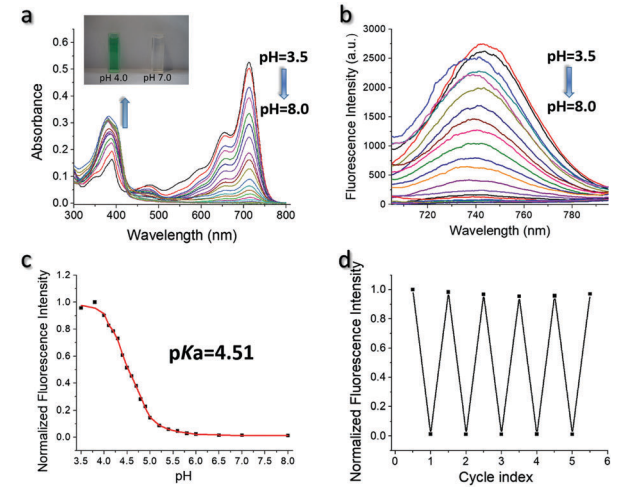

Fig. 1 (a) UV-Vis spectra of 10 μM **NRH-Lyso** in BR buffer with varying pH values. Insert: Photos of the BR solutions with different pH: left 7.0 and right 4.0. (b) Fluorescence spectra of 10 μM **NRH-Lyso** in BR buffer with varying pH values, excitation: 808 nm laser. (c) Plots of normalized fluorescence intensity *vs.* pH (pK_a = 4.51). (d) pH reversibility study of **NRH-Lyso** in BR buffer at two different pH values (4.0 and 7.0).

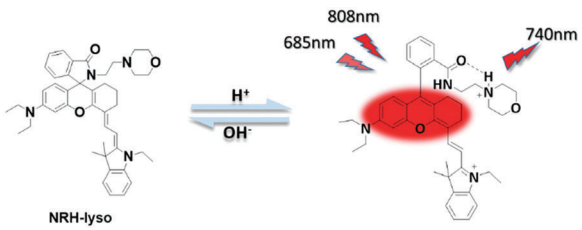

Scheme 2 Response mechanism of **NRH-Lyso** to acidic pH, and a schematic of its FUCL.

(R^2 = 0.99397) of luminescence intensity *versus* pH value in the range of 4.0–5.0 (Fig. S2, ESI†). **NRH-Lyso** also showed good reversibility between pH 4.0 and 7.0. We then investigated the underlying mechanism of upconversion emission in **NRH-Lyso** under 808 nm laser excitation. As shown in Fig. S3 (ESI†), the luminescence intensity of **NRH-Lyso** showed excellent linearity (R^2 = 0.99837) with excitation power ranging from 0.1 W to 0.7 W; this indicated that the luminescence form of **NRH-Lyso** excited at 808 nm belonged to a single and not a multiple process.[55,61,63,64,68] We then explored the relationship between luminescence intensity and temperature. As shown in Fig. S4 (ESI†), the normalized fluorescence intensity increased when the temperature increased.[61,63,64,67–69] Thus, we can conclude that this type of luminescence in **NRH-Lyso** occurring under 808 nm laser excitation is frequency upconversion. To further investigate the spectroscopic properties of **NRH-Lyso**, different experiments including pH titration and time response experiments under 685 nm excitation were also performed, where we also observed the same variation under 685 nm excitation. The results showed good coherence with the results, such as excellent linearity in the pH range of 4.0–4.8 and the same phenomena, obtained under 808 nm excitation (Fig. S6–S9, ESI†).

As shown in Fig. 2, the fluorescence intensity at both 685 nm and 808 nm excitation of **NRH-Lyso** at pH 7.0 and pH 4.0

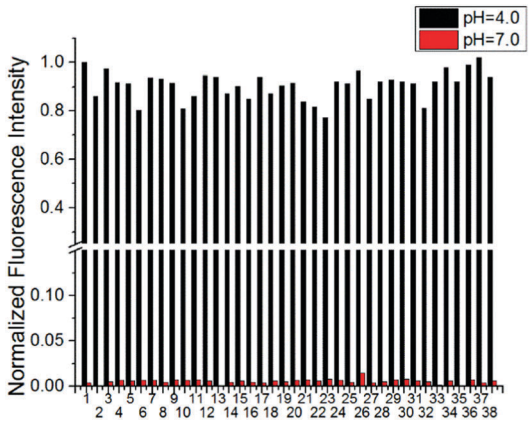

Fig. 2 Fluorescence responses of the **NRH-Lyso** probe (10 μM) to different potential interfering agents in pH 4.0 and 7.0 BR buffer solutions. (E_x = 808 nm 1. Control, 2. Ag^+, 3. Al^{3+}, 4. Ca^{2+}, 5. Cd^{2+}, 6. Co^{2+}, 7. Cr^{3+}, 8. Cu^{2+}, 9. Fe^{3+}, 10. Hg^{2+}, 11. K^+, 12. Li^+, 13. Mg^{2+}, 14. Mn^{2+}, 15. Na^+, 16. Ni^{2+}, 17. Pb^{2+}, 18. Zn^{2+}, 19. Arg, 20. Asp, 21. Cys, 22. Glu, 23. GSH, 24. Hcy, 25. His, 26. Leu, 27. Lys, 28. Ser, 29. Thr, 30. Trp, 31. Tyr, 32. Val, 33. Ac^-, 34. CO_3^{2-}, 35. $H_2PO_4^-$, 36. HPO_4^{2-}, 37. Glucose and 38. H_2O_2).

showed negligible changes in the presence of common cations such as Na^+, K^+, Li^+, Ca^{2+}, and Mg^{2+}, heavy and transition-metal ions, such as Hg^{2+}, Cd^{2+}, Co^{2+}, Ni^{2+}, Zn^{2+}, Mn^{2+}, Cu^{2+}, Pb^{2+}, Ag^+, Al^{3+}, Cr^{3+} and Fe^{3+}, HPO_4^{2-}, CO_3^{2-}, and various biological molecules including amino acids, glucose, and reactive oxygen species (HClO and H_2O_2), which exhibited negligible interference in the fluorescence of **NRH-Lyso**. In addition, the fluorescence intensity of **NRH-Lyso** generally remained stable in the presence of common anions (Ac^- and $H_2PO_4^-$). Moreover, the aforementioned analytes had little influence on the fluorescence intensity of **NRH-Lyso** at pH = 4.0. The same results were obtained under 685 nm excitation (Fig. S10, ESI†). These results demonstrate that **NRH-Lyso** exhibits a specific fluorescence response to acidic pH with negligible interference from other analytes.

Fluorescence imaging in living cells

To evaluate the potential biological applications of **NRH-Lyso** in living samples, cell imaging experiments were performed on RAW 264.7 cells using confocal laser scanning microscopy (CLSM). We first performed imaging experiments using RAW 264.7 cells at different times under 808 nm laser excitation. As shown in Fig. 3, the fluorescence intensity in the cytoplasm almost reached saturation in 30 min.

Bright spots with NIR fluorescence could be observed in the cytoplasm near the perinuclear regions of the live RAW 264.7 cells. Then, imaging experiments on RAW 264.7 cells stained with different concentrations of **NRH-Lyso** were also performed. After 30 min incubation, clear NIR fluorescence of **NRH-Lyso** was detected at concentrations as low as 5 μM (ESI,† S11). These two abovementioned results demonstrate that the **NRH-Lyso** probe can penetrate the cell membrane in a certain period; thus, we have chosen 30 min and 10 μM as the best incubation time and concentration in the following tests, respectively.

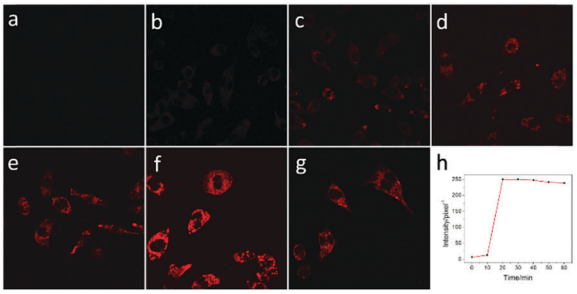

Fig. 3 CLSM images of the RAW 264.7 cells stained with **NRH-Lyso** (10 μM) at different times. (a–g) 0 min, 10 min, 20 min, 30 min, 40 min, 50 min and 60 min. (h) Average fluorescence intensity of each sample at different times.

4-(2-Aminoethyl) morpholine is a well-used lysosome targeting functional group.[70,71] Therefore, we introduced it into our luminescence functional group **NRH** as the targeting site such that **NRH-Lyso** could selectively stain lysosomes in living cells. Consequently, colocalization experiments with the commercial lysosome dye LysoTracker Green DND-26 (LTG) were conducted to identify the intracellular location of **NRH-Lyso**. As shown in Fig. 4, **NRH-Lyso** shows red luminescence under 808 nm laser excitation, and LTG exhibits green fluorescence under 488 nm excitation in living cells. The overlap between the red and green fluorescence images was studied to evaluate the organelle locating ability of our probe. **NRH-Lyso** and LTG had nearly the same distribution in the living RAW 264.7 cells. In the final results, the corresponding coefficient was 0.95. The abovementioned imaging test data demonstrates that **NRH-Lyso** is a good candidate for selectively locating lysosomes in living cells.

Furthermore, we tested the ability of **NRH-Lyso** to sense cellular pH values in living cells. RAW 264.7 cells were incubated with **NRH-Lyso** (10 μM) for 30 min, and the incubating media were replaced by PBS buffer containing 10 μM nigericin and 5 μM monensin at different pH values (pH 4.0, 4.5, 5.0, 5.5, 6.0, and 7.0). After incubation for another 30 min, the cell culture

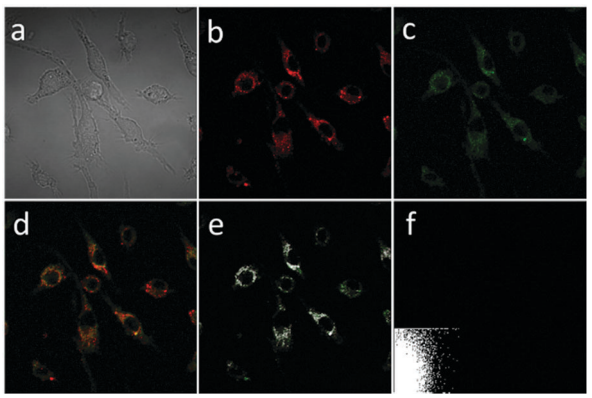

Fig. 4 CLSM images of the RAW 264.7 cells stained with **NRH-Lyso** (10 μM) and LTG (100 nM). (a) Bright-field image. (b) Fluorescence image of **NRH-Lyso** in the Cy5 channel. (c) Fluorescence image of **NRH-Lyso** in the FITC channel. (d and e) Overlay of (a), (b), and (c). (f) Fluorescence intensity correlation plot of **NRH-Lyso** (Cy5 channel) and LTG (FITC channel).

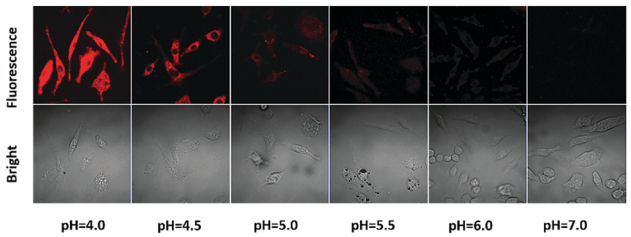

Fig. 5 CLSM images of the RAW 264.7 cells stained with **NRH-Lyso** (10 μM) in different pH BR buffer.

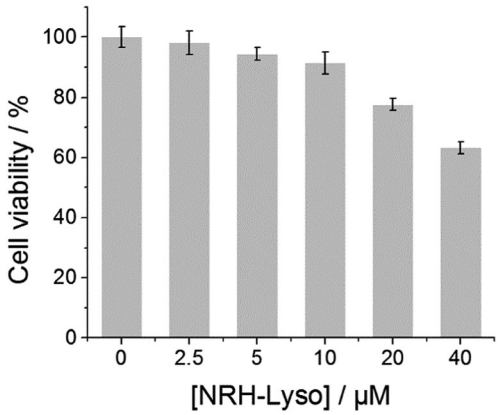

Fig. 6 Cytotoxicity of **NRH-Lyso** in RAW 264.7 cells.

plates were washed with the corresponding PBS buffer three times before cell imaging was performed. The NIR fluorescence intensity of **NRH-Lyso** in the living cells decreased from pH 4.0 to 7.0 due to the formation of the spirolactam **NRH-Lyso**, which showed no fluorescence (Fig. 5). Hardly any fluorescence could be detected in the RAW 264.7 cells at a pH of 6.0. It should be noted that the NIR fluorescence of **NRH-Lyso** was distributed throughout the cell; however, this abnormal phenomenon was also observed in the literature.

All these data indicate that **NRH-Lyso** exhibits good sensitivity during lysosome pH changes monitored in living cells.

Cytotoxicity

A standard MTT experiment was employed to evaluate the cytotoxicity of this probe in living cells. After incubation at 37 °C for 24 h, the cell viabilities of the RAW 264.7 cells were relatively high (Fig. 6). The cell viability was maintained at above 90% at the concentration used in the abovementioned experiments. Even when the concentration of **NRH-Lyso** was increased to 20 μM, the cell viability was still higher than 77%. Therefore, **NRH-Lyso** exhibits very low cytotoxicity.

Conclusions

In conclusion, we synthesized a novel lysosomal pH monitoring probe, **NRH-Lyso**, based on the rhodamine derivative **NRH**. **NRH-Lyso** showed great frequency upconversion luminescence response (740 nm) to acidic pH due to the H^+-induced ring opening non-fluorescence form of **NRH** and could specifically recognize lysosomes in living cells. By conjugating the lysosome targeting group 4-(2-aminoethyl)morpholine with **NRH**, the probe could specifically recognize lysosomes in living cells. Furthermore, **NRH-Lyso** exhibits a suitable pH detection range (pK_a = 4.51), high sensitivity, good selectivity, good reversibility, excellent photostability, and low cytotoxicity. **NRH-Lyso** was successfully used for imaging lysosomal pH in live cells. The present study provides a general platform for the development of a series of frequency upconversion rhodamine-based probes and organelle targeting probes for the detection and imaging of a wide range of analytes in living samples.

Conflicts of interest

There are no conflicts of interest to declare.

Acknowledgements

This study was supported by the NSFC (Grant 21431002).

Notes and references

1 J. R. Casey, S. Grinstein and J. Orlowski, *Nat. Rev. Mol. Cell Biol.*, 2010, **11**, 50.
2 R. Martínez-Zaguilán, B. F. Chinnock, S. Wald-Hopkins, M. Bernas, D. Way, M. Weinand, M. H. Witte and R. J. Gillies, *Cell. Physiol. Biochem.*, 1996, **6**, 169.
3 R. A. Gottlieb, J. Nordberg, E. Skowronski and B. M. Babior, *Proc. Natl. Acad. Sci. U. S. A.*, 1996, **93**, 654.
4 A. Ishaque and M. Al-Rubeai, *J. Immunol. Methods*, 1998, **221**, 43.
5 M. Lakadamyali, M. J. Rust, H. P. Babcock and X. Zhuang, *Proc. Natl. Acad. Sci. U. S. A.*, 2003, **100**, 9280.
6 A. P. Lieberman, R. Puertollano, N. Raben, S. Slaugenhaupt, S. U. Walkley and A. Ballabio, *Autophagy*, 2012, **8**, 719.
7 X. D. Liu, Y. Xu, R. Sun, Y. J. Xu, J. M. Lu and J. F. Ge, *Analyst*, 2013, **138**, 6542.
8 R. Khazen, S. Muller, N. Gaudenzio, E. Espinosa, M. P. Puissegur and S. Valitutti, *Nat. Commun.*, 2016, **7**, 15.
9 E. Kadar, S. A. Davis and A. Lobo-da-Cunha, *J. Mar. Biol.*, 2008, **153**, 995.
10 K. A. Christensen, J. T. Myers and J. A. Swanson, *J. Cell Sci.*, 2002, **115**, 599.
11 J. Stinchcombe, G. Bossi and G. M. Griffiths, *Science*, 2004, **305**, 55.
12 H. Zhu, J. Fan, Q. Xu, H. Li, J. Wang, P. Gao and X. Peng, *Chem. Commun.*, 2012, **48**, 11766.
13 H. Izumi, T. Torigoe, H. Ishiguchi, H. Uramoto, Y. Yoshida, M. Tanabe, T. Ise, T. Murakami, T. Yoshida, M. Nomoto and K. Kohno, *Cancer Treat. Rev.*, 2003, **29**, 541.
14 M. Barrachina, T. Maes, C. Buesa and I. Ferrer, *Neuropathol. Appl. Neurobiol.*, 2006, **32**, 505.
15 X. K. Cui, H. Y. Liu, J. Li, K. W. Guo, W. X. Han, Y. Dong, S. M. Wan, X. C. Wang, P. P. Jia, S. L. Li, Y. F. Ma, J. Zhang,

H. M. Mu and Y. Z. Hu, *Int. J. Biochem. Cell Biol.*, 2016, **79**, 118.
16 S. F. Piao, R. K. Amaravadi and S. New York Acad, in *Targeting the Lysosome*, Blackwell Science Publ, Oxford, 2016, vol. 1371, pp. 45.
17 M. H. Lee, N. Park, C. Yi, J. H. Han, J. H. Hong, K. P. Kim, D. H. Kang, J. L. Sessler, C. Kang and J. S. Kim, *J. Am. Chem. Soc.*, 2014, **136**, 14136.
18 B. L. Dong, X. Z. Song, C. Wang, X. Q. Kong, Y. H. Tang and W. Y. Lin, *Anal. Chem.*, 2016, **88**, 4085.
19 Y. H. Li, Y. J. Wang, S. Yang, Y. R. Zhao, L. Yuan, J. Zheng and R. H. Yang, *Anal. Chem.*, 2015, **87**, 2495.
20 H. S. Lv, J. Liu, J. Zhao, B. X. Zhao and J. Y. Miao, *Sens. Actuators, B*, 2013, **177**, 956.
21 Q. Wan, S. Chen, W. Shi, L. Li and H. Ma, *Angew. Chem., Int. Ed.*, 2014, **53**, 10916.
22 Q. A. Best, R. S. Xu, M. E. McCarroll, L. C. Wang and D. J. Dyer, *Org. Lett.*, 2010, **12**, 3219.
23 X. F. Zhang, T. Zhang, S. L. Shen, J. Y. Miao and B. X. Zhao, *J. Mater. Chem. B*, 2015, **3**, 3260.
24 B. Tang, F. Yu, P. Li, L. L. Tong, X. Duan, T. Xie and X. Wang, *J. Am. Chem. Soc.*, 2009, **131**, 3016.
25 H. J. Kim, C. H. Heo and H. M. Kim, *J. Am. Chem. Soc.*, 2013, **135**, 17969.
26 J. Kneipp, H. Kneipp, B. Wittig and K. Kneipp, *Nano Lett.*, 2007, **7**, 2819.
27 D. G. Smith, B. K. McMahon, R. Pal and D. Parker, *Chem. Commun.*, 2012, **48**, 8520.
28 B. Dong, X. Song, C. Wang, X. Kong, Y. Tang and W. Lin, *Anal. Chem.*, 2016, **88**, 4085.
29 Z. Guo, S. Park, J. Yoon and I. Shin, *Chem. Soc. Rev.*, 2014, **43**, 16.
30 J. Han and K. Burgess, *Chem. Rev.*, 2010, **110**, 2709.
31 J. T. Hou, W. X. Ren, K. Li, J. Seo, A. Sharma, X. Q. Yu and J. S. Kim, *Chem. Soc. Rev.*, 2017, **46**, 2076.
32 Y. Ni and J. Wu, *Org. Biomol. Chem.*, 2014, **12**, 3774.
33 M. Schäferling, *Wiley Interdiscip. Rev.: Nanomed. Nanobiotechnol.*, 2016, **8**, 378.
34 W. Shi, X. Li and H. Ma, *Methods Appl. Fluoresc.*, 2014, **2**, 042001.
35 R. Wang, C. Yu, F. Yu, L. Chen and C. Yu, *TrAC, Trends Anal. Chem.*, 2010, **29**, 1004.
36 W. Xu, Z. Zeng, J.-H. Jiang, Y.-T. Chang and L. Yuan, *Angew. Chem., Int. Ed.*, 2016, **55**, 13658.
37 J. Yin, Y. Hu and J. Yoon, *Chem. Soc. Rev.*, 2015, **44**, 4619.
38 Y. Yue, F. Huo, S. Lee, C. Yin and J. Yoon, *Analyst*, 2016, **142**, 30.
39 R. Zhang, F. Yan, Y. Huang, D. Kong, Q. Ye, J. Xu and L. Chen, *RSC Adv.*, 2016, **6**, 50732.
40 J. Zhou and H. Ma, *Chem. Sci.*, 2016, **7**, 6309.
41 G. K. Vegesna, J. Janjanam, J. Bi, F.-T. Luo, J. Zhang, C. Olds, A. Tiwari and H. Liu, *J. Mater. Chem. B*, 2014, **2**, 4500.
42 M. Yu, X. Wu, B. Lin, J. Han, L. Yang and S. Han, *Anal. Chem.*, 2015, **87**, 6688.
43 S. Zhang, T.-H. Chen, H.-M. Lee, J. Bi, A. Ghosh, M. Fang, Z. Qian, F. Xie, J. Ainsley, C. Christov, F.-T. Luo, F. Zhao and H. Liu, *ACS Sens.*, 2017, **2**, 924.
44 J. Zhang, M. Yang, C. Li, N. Dorh, F. Xie, F.-T. Luo, A. Tiwari and H. Liu, *J. Mater. Chem. B*, 2015, **3**, 2173.
45 R. Sun, W. Liu, Y.-J. Xu, J.-M. Lu, J.-F. Ge and M. Ihara, *Chem. Commun.*, 2013, **49**, 10709.
46 L. Fan, Y.-J. Fu, Q.-L. Liu, D.-T. Lu, C. Dong and S.-M. Shuang, *Chem. Commun.*, 2012, **48**, 11202.
47 Q. Wan, S. Chen, W. Shi, L. Li and H. Ma, *Angew. Chem.*, 2014, **126**, 11096.
48 B. Liu, Y. Y. Chen, C. X. Li, F. He, Z. Y. Hou, S. S. Huang, H. M. Zhu, X. Y. Chen and J. Lin, *Adv. Funct. Mater.*, 2015, **25**, 4717.
49 W. Fan, W. Bu, B. Shen, Q. He, Z. Cui, Y. Liu, X. Zheng, K. Zhao and J. Shi, *Adv. Mater.*, 2015, **27**, 4155.
50 B. Tian, Q. Wang, Q. Su, W. Feng and F. Li, *Biomaterials*, 2017, **112**, 10.
51 X. H. Wang, H. J. Chang, J. Xie, B. Z. Zhao, B. T. Liu, S. L. Xu, W. B. Pei, N. Ren, L. Huang and W. Huang, *Coord. Chem. Rev.*, 2014, **273**, 201.
52 R. Arppe, T. Nareoja, S. Nylund, L. Mattsson, S. Koho, J. M. Rosenholm, T. Soukka and M. Schaferling, *Nanoscale*, 2014, **6**, 6837.
53 S. Du, J. Hernandez-Gil, H. Dong, X. Zheng, G. Lyu, M. Banobre-Lopez, J. Gallo, L.-d. Sun, C.-h. Yan and N. J. Long, *Dalton Trans.*, 2017, **46**, 13957.
54 H. Li, H. Dong, M. Yu, C. Liu, Z. Li, L. Wei, L.-D. Sun and H. Zhang, *Anal. Chem.*, 2017, **89**, 8863.
55 Y. Liu, Q. Su, M. Chen, Y. Dong, Y. Shi, W. Feng, Z. Y. Wu and F. Li, *Adv. Mater.*, 2016, **28**, 6625.
56 X. Zhu, Q. Su, W. Feng and F. Li, *Chem. Soc. Rev.*, 2017, **46**, 1025.
57 M. Albota, D. Beljonne, J.-L. Brédas, J. E. Ehrlich, J.-Y. Fu, A. A. Heikal, S. E. Hess, T. Kogej, M. D. Levin, S. R. Marder, D. McCord-Maughon, J. W. Perry, Harald Rockel, M. Rumi, G. Subramaniam, W. W. Webb, X.-L. Wu and C. Xu, *Science*, 1998, **281**, 1653.
58 M. Pawlicki, H. A. Collins, R. G. Denning and H. L. Anderson, *Angew. Chem., Int. Ed.*, 2009, **48**, 3244.
59 B. Stevens, *Chem. Rev.*, 1957, **57**, 439.
60 S. Kumazaki, *Chem. Phys.*, 2013, **419**, 107.
61 D. Bloor, G. Cross, P. K. Sharma, J. A. Elliott and G. Rumbles, *J. Chem. Soc., Faraday Trans.*, 1993, **89**, 4013.
62 R. W. Wood, *Philos. Mag.*, 1928, **6**, 310.
63 J. L. Clark and G. Rumbles, *Phys. Rev. Lett.*, 1996, **76**, 2037.
64 J. L. Clark, P. F. Miller and G. Rumbles, *J. Phys. Chem. A*, 1998, **102**, 4428.
65 A. N. Kuzmin, A. Baev, A. V. Kachynski, T. S. Fisher, A. Shakouri and P. N. Prasad, *J. Appl. Phys.*, 2011, **110**, 033512.
66 H. Yang, C. Han, X. Zhu, Y. Liu, K. Y. Zhang, S. Liu, Q. Zhao, F. Li and W. Huang, *Adv. Funct. Mater.*, 2016, **26**, 1945.
67 Y. Liu, Q. Su, X. Zou, M. Chen, W. Feng, Y. Shi and F. Li, *Chem. Commun.*, 2016, **52**, 7466.
68 M. H. Bartl, B. J. Scott, G. Wirnsberger, A. Popitsch and G. D. Stucky, *ChemPhysChem*, 2003, **4**, 392.
69 A. V. Kachynski, A. N. Kuzmin, H. E. Pudavar and P. N. Prasad, *Appl. Phys. Lett.*, 2005, **87**, 023901.
70 W. Luo, H. Jiang, X. Tang and W. Liu, *J. Mater. Chem. B*, 2017, **5**, 4768.
71 G. Niu, P. Zhang, W. Liu, M. Wang, H. Zhang, J. Wu, L. Zhang and P. Wang, *Anal. Chem.*, 2017, **89**, 1922.

